



**HAL**  
open science

# Magnetic ordering and anomalous ground state in CeAl 2

B. Barbara, M. F. Rossignol, J. X Boucherle, J. Schweizer, J. L. L Buevoz

► **To cite this version:**

B. Barbara, M. F. Rossignol, J. X Boucherle, J. Schweizer, J. L. L Buevoz. Magnetic ordering and anomalous ground state in CeAl 2. Journal of Applied Physics, American Institute of Physics, 1979, 50 (B3), pp.2300 - 2307. 10.1063/1.327036 . hal-01659998

**HAL Id: hal-01659998**

**<https://hal.archives-ouvertes.fr/hal-01659998>**

Submitted on 9 Dec 2017

**HAL** is a multi-disciplinary open access archive for the deposit and dissemination of scientific research documents, whether they are published or not. The documents may come from teaching and research institutions in France or abroad, or from public or private research centers.

L'archive ouverte pluridisciplinaire **HAL**, est destinée au dépôt et à la diffusion de documents scientifiques de niveau recherche, publiés ou non, émanant des établissements d'enseignement et de recherche français ou étrangers, des laboratoires publics ou privés.

## Magnetic ordering and anomalous ground state in CeAl<sub>2</sub>

B. Barbara, M. F. Rossignol, J. X. Boucherle, J. Schweizer, and J. L. Buevoz

Citation: *Journal of Applied Physics* **50**, 2300 (1979); doi: 10.1063/1.327036

View online: <http://dx.doi.org/10.1063/1.327036>

View Table of Contents: <http://scitation.aip.org/content/aip/journal/jap/50/B3?ver=pdfcov>

Published by the [AIP Publishing](#)

---

### Articles you may be interested in

Generation and reactivity of putative support systems, Ce-Al neutral binary oxide nanoclusters: CO oxidation and C-H bond activation

*J. Chem. Phys.* **139**, 194313 (2013); 10.1063/1.4830406

Anomalous magnetic ground state in PrSi evidenced by the magnetocaloric effect

*J. Appl. Phys.* **111**, 07A943 (2012); 10.1063/1.3679415

Low temperature transport properties of Ce-Al metallic glasses

*J. Appl. Phys.* **109**, 113716 (2011); 10.1063/1.3587453

Dynamical properties of quantum spin systems in magnetically ordered product ground states

*J. Appl. Phys.* **75**, 6057 (1994); 10.1063/1.355509

NMR in CeAl<sub>2</sub>: Crystalfield effects and magnetic order in the lowtemperature phase

*J. Appl. Phys.* **49**, 2121 (1978); 10.1063/1.324758

---

An advertisement for Asylum Research Cypher AFMs. The background is dark blue with a film strip graphic on the left. The text is in white and orange. The Oxford Instruments logo is in the bottom right corner.

**Not all AFMs are created equal**  
**Asylum Research Cypher™ AFMs**  
**There's no other AFM like Cypher**

[www.AsylumResearch.com/NoOtherAFMLikeIt](http://www.AsylumResearch.com/NoOtherAFMLikeIt)

**OXFORD**  
INSTRUMENTS  
*The Business of Science®*

# Magnetic ordering and anomalous ground state in $\text{CeAl}_2$

B. Barbara and M. F. Rossignol

Laboratoire Louis Néel, C.N.R.S., 166X, 38042 Grenoble-cédex, France

J. X. Boucherle and J. Schweizer<sup>+</sup>

D.R.F./D.N., Centre d'Etudes Nucléaires, 85X, 38041 Grenoble-cédex, and <sup>+</sup>Institut Laue-Langevin, 156X, 38042 Grenoble-cédex, France

J. L. Buevoz

Institut Laue-Langevin, 156X, 38042 Grenoble-cédex, France

The intermetallic Laves phase compound  $\text{CeAl}_2$  presents some unusual properties, which makes the exact nature of its ground state a matter of great interest. A first step towards an explanation would be the knowledge of any magnetic structure below 3.8 K (phase transition temperature). We have carried out very accurate neutron diffraction experiments on a polycrystalline sample, completed by experiments on a single crystal. Several magnetic reflections have been found which are characteristic of the propagation vector  $\vec{k} = 1/2 + \tau, 1/2 - \tau, 1/2$ . The corresponding magnetic structure consists of antiferromagnetic ( $1\bar{1}0$ ) planes in which the magnetic moments, lying along  $[111]$ , are modulated according to a sine wave propagation along  $[1\bar{1}0]$ . No variation of  $\vec{k}$  nor any tendency towards antiphase structure appear down to 0.4 K. This result is not coherent with the Kramers' degeneracy of the  $\text{Ce}^{3+}$  ion because it implies a non magnetic level as a ground state. On the other hand previous polarized neutron experiments have shown an antiparallel coupling between the spins of the cerium and the conduction electrons. Both results, as well as other physical properties, agree with the existence of a singlet ground state associated with a strong d-f coupling.

PACS numbers: 75.25.+z, 75.30.Kz

## INTRODUCTION

The Kondo effect was introduced first [1] to explain the resistivity minimum in dilute alloys. It has been extended recently to the case of concentrated systems. In particular there is evidence of such an effect in the compound  $\text{CeAl}_2$  [2,3].

At temperatures where concentrated magnetic alloys usually undergo a phase transition towards a magnetic order, the Kondo effect in dilute systems results in a vanishing of the magnetic moments. It is therefore interesting to study what happens to concentrated Kondo systems when the temperature decreases to zero. This paper first summarizes neutron diffraction experiments which give an answer to this question in the case of  $\text{CeAl}_2$ . With the help of the experimental results it then discusses some of the peculiar properties of this compound.

## I. NATURE OF THE MAGNETIZATION

The magnetization of a  $\text{CeAl}_2$  single crystal was measured at the S.N.C.I. in fields up to 150 kOe for the different orientations  $[100]$ ,  $[110]$  and  $[111]$  of the crystal [4]. The magnetization is anisotropic and shows different qualitative behaviours above and below 3.8 K. Above this temperature the magnetization increases steadily with increasing field. Below 3.8 K the magnetization curves present an inflexion point most pronounced at the lowest temperatures, characteristic of a metamagnetic type behaviour (fig. 1). In larger fields the behaviour is typically paramagnetic. The variation of the position of the inflexion point in the field-temperature plane corresponds to the boundary between the paramagnetic phase and a low temperature phase which will be shown later to be ordered. This curve is presented as an insert in figure 1 for the field along  $[111]$ . Such a phase boundary was

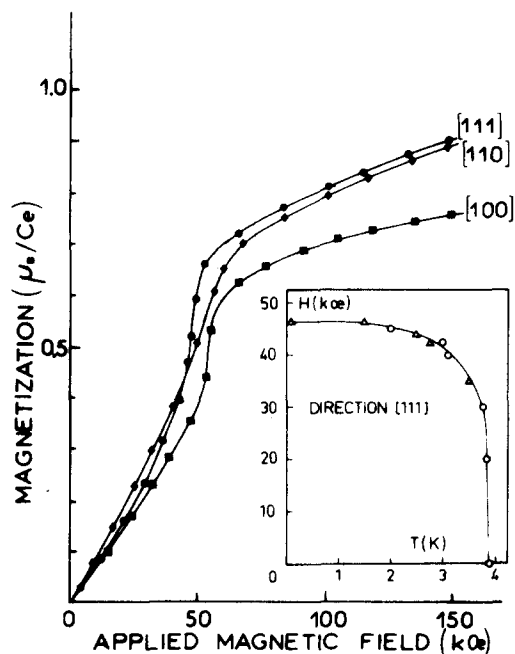


Fig. 1 Magnetization curves measured along the three principal directions in a single crystal of  $\text{CeAl}_2$  at 1.7 K [4]. The insert shows the variation of the threshold field for the direction  $[111]$  obtained from magnetization curves (triangles) [4] and from specific heat measurements (circles) [6].

also determined from specific heat [5,6] and dilatation measurements [7] under magnetic fields.

In the cubic crystal field the sixfold degeneracy of  $Ce^{3+}$  ( $J = 5/2$ ) splits into a quartet  $\Gamma_8$  and a doublet  $\Gamma_7$ . The value of the magnetization at low temperature extrapolated from high fields to  $H = 0$  indicates that the ground state is the doublet [4]. This confirms previous specific heat results [8].

However, several neutron experiments were unable to observe any magnetic ordering. In order to throw some light on the nature of magnetism in  $CeAl_2$ , a study of the magnetization density around the cerium atoms was undertaken.

This study was performed with the sensitivity of polarized neutrons and using an applied magnetic field to induce a ferromagnetic component. One defines for each Bragg reflection of the crystal structure, a magnetic structure factor  $F_M(hkl)$  besides the nuclear structure factor  $F_N(hkl)$ .

The intensities of the Bragg reflections for the two possible polarization directions of the beam are :

$$I^\pm(hkl) = F_N^2(hkl) \pm 2F_N(hkl)F_M(hkl) + F_M^2(hkl)$$

From the flipping ratio  $R(hkl) = I^+(hkl)/I^-(hkl)$  one deduces the value  $\gamma(hkl) = F_M(hkl)/F_N(hkl)$  and then, knowing  $F_N(hkl)$  from the crystal structure, one obtains  $F_M(hkl)$  with a high accuracy.

The experiment was carried out on the polarized neutron diffractometer D5 of the high flux reactor of the I.L.L. A 48 kOe vertical field, provided by a superconducting Helmholtz split coil, was applied along either the  $[001]$  axis or the  $[01\bar{1}]$  axis of a  $CeAl_2$  single crystal cooled down to a temperature of 1.5 K. The data have been corrected for imperfect polarization and  $\lambda/2$  contamination of the neutron beam. Extinction corrections have also been carried out taking advantage of the short wavelength provided by D5.

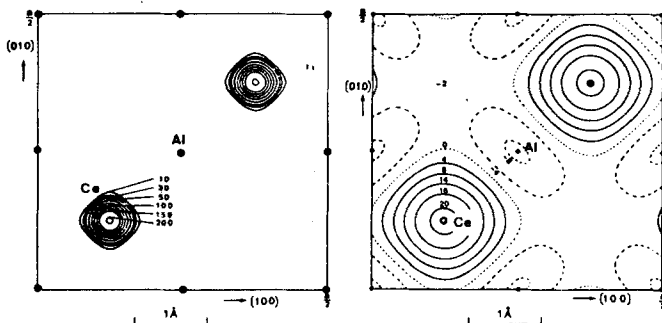


Fig. 2 Magnetization densities in  $CeAl_2$  projected on the (001) plane (in  $10^{-3} \mu_B/\text{\AA}^2$ ): the left part is the total density (a) and the right part the difference between the total and the 4f densities (b). (The errors are about  $5 \cdot 10^{-3} \mu_B/\text{\AA}^2$ ).

The magnetic structure factors were measured in the horizontal plane of the diffractometer. Thus by Fourier transformation of these data, one can obtain the projection of the magnetization density onto the basal plane for the two experiments. The density maps show that the magnetization is mainly localized around the cerium nuclei (for the (001) plane the map is presented in figure 2a). This result allows an analysis of the magnetic structure factors in an ionic model using tensor operator methods [9]. In this approach the structure factors are related to the angular wave function of the 4f shell,  $|\psi\rangle = \sum_M a_M |J, M\rangle$ , using i) quantities which depend only on the 4f electron configuration in the free ion (tabulated for rare earths in reference 10), and ii) the radial integrals which depend on the radial part of the wave function (calculated for the free ion with the relativistic Dirac Fock method [11]). In the case of  $Ce^{3+}$  ion in  $CeAl_2$  the degeneracy of the  $\Gamma_7$  crystal field ground

state is removed by the exchange and applied fields, and the wave functions of the resulting ground states are, for the two orientations of the field :

$$\begin{aligned} \Psi[001] &= a_{3/2} |5/2, 3/2\rangle + a_{-5/2} |5/2, -5/2\rangle \\ \Psi[01\bar{1}] &= a'_{5/2} |5/2, 5/2\rangle + a'_{1/2} |5/2, 1/2\rangle \\ &\quad + a'_{-3/2} |5/2, 3/2\rangle \end{aligned}$$

It is therefore easy to determine the values of  $a_M$  which give the best fit to the observed magnetic amplitudes for each of the two cases [12]. As the moments are polarized by the applied field a normalization factor has to be refined too. The wave functions obtained are (for the two ground states) :

$$\begin{aligned} \Psi[001] &= 0.945(12) |5/2, 3/2\rangle - 0.328(35) |5/2, -5/2\rangle \\ \Psi[01\bar{1}] &= 0.691(6) |5/2, 5/2\rangle - 0.627(10) |5/2, 1/2\rangle \\ &\quad - 0.358(21) |5/2, -3/2\rangle \end{aligned}$$

Such wave functions, with similar coefficients, can be obtained also by a direct diagonalization of an Hamiltonian consisting of crystal field, external and exchange fields [12], if one assumes an exchange field of about 75 kOe.

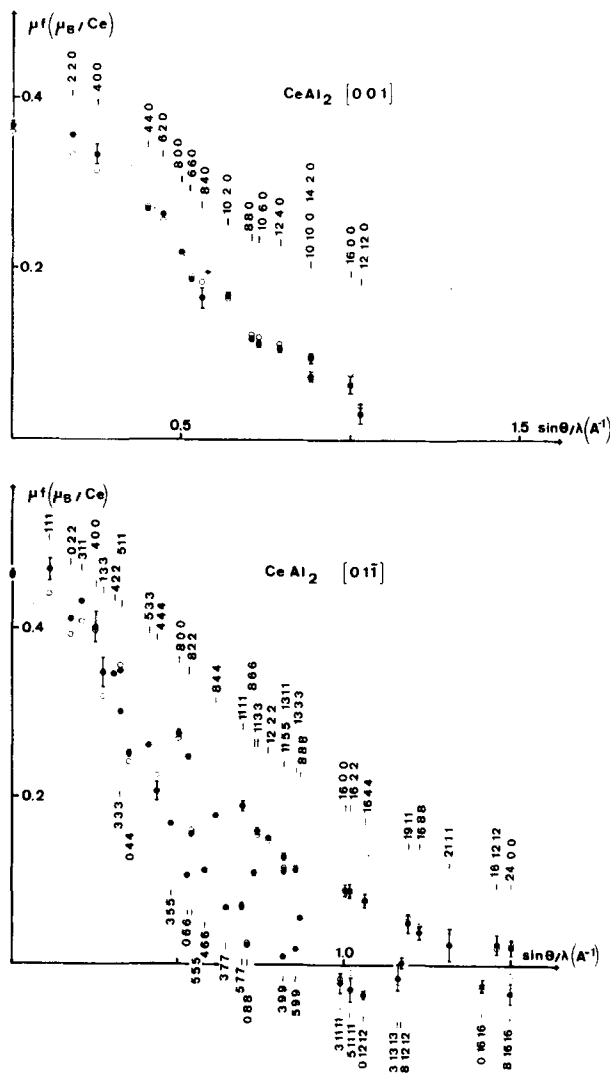


Fig. 3 Form factors of  $CeAl_2$  with field applied along  $[001]$  (upper part) and  $[01\bar{1}]$  (lower part). The full circles are experimental values and the open circles are the calculated ones.

The agreement between calculated and observed values for the magnetic structure factors (figure 3) is very good, especially considering the enormous scatter-

ring of points when the field is parallel to  $[01\bar{1}]$ . The only discrepancies occur for reflections corresponding to low values of  $\sin \theta/\lambda$ . Such discrepancies have already been found in gadolinium [13],  $\text{NdAl}_2$  [14] and  $\text{HoAl}_2$  [15]. They indicate that beside the 4f magnetization density there exists a more diffuse density which varies slowly throughout the cell. The corresponding density map can be obtained by a Fourier transformation of the difference between the observed structure factors and the values calculated for the 4f electrons. Such a map is presented on figure 2b for the (001) projection. For the two cases, the density shows a positive contribution around the cerium atoms, which is more expanded than the 4f shell. Most of this density can be attributed to electrons of 5d character. The polarization of these electrons is due to the spin  $S$  of the 4f shell. It is very interesting to compare the sign and the magnitude of this polarization in different rare earth systems. Such a comparison appears in table I which gives values of the diffuse magnetization density at the rare earth position. As the coupling between  $\vec{J}$  and  $\vec{S}$  changes from the first to the second half of the series one expects a change of sign for the diffuse magnetization. Indeed such a change is observed, but one can see that cerium does not behave like the other rare earths : one expects a negative magnetization as in  $\text{NdAl}_2$ , but the contrary is observed. This discrepancy can be attributed to a change of the exchange coupling  $\vec{J}$  between the 4f spins  $\vec{S}$  and conduction electrons spins  $\vec{s}$ .

TABLE I

Diffuse magnetization densities at the rare earth site. Values in  $\mu_B/\text{\AA}^2$  correspond to a projection. The factor  $(g_J - 1)$  is also given ( $\vec{S} = (g_J - 1)\vec{J}$ ).

System	Value of $\rho_D$	$g_J - 1$
$\text{CeAl}_2$ [001]	0.020 (8) $\mu_B/\text{\AA}^2$	-1/7
$\text{CeAl}_2$ $[01\bar{1}]$	0.043(15) $\mu_B/\text{\AA}^2$	-1/7
$\text{NdAl}_2$ [001]	-0.09 (2) $\mu_B/\text{\AA}^2$	-3/11
	-0.030 (5) $\mu_B/\text{\AA}^3$	
$\text{HoAl}_2$ $[01\bar{1}]$	1.60 (20) $\mu_B/\text{\AA}^2$	+1/4
Gd	0.056(12) $\mu_B/\text{\AA}^3$	+ 1

This study of the magnetization distribution in  $\text{CeAl}_2$  clearly shows that most of it is due to the 4f electrons of trivalent cerium atoms whose wave function can be determined in a very classical way. There is in addition a more diffuse magnetization due to the polarization of conduction electrons of d character by the 4f spins. Contrarily to the other rare earth the coupling constant is negative in  $\text{CeAl}_2$ . This constitutes a direct observation of the negative coupling already established by indirect means in several Ce compounds [2,16,17,3].

## II. DETERMINATION OF THE MAGNETIC STRUCTURE

In order to investigate further the magnetic properties, we have determined the magnetic structure by classical neutron diffraction. An experiment on a powder allows observation of all directions of the reciprocal space in a single pattern. But due to the low value of the  $\text{Ce}^{3+}$  moment a very sensitive apparatus was necessary. Such an apparatus allowed us to observe very weak magnetic lines. Following these results more accurate measurements were possible using a single crystal, and the structure was completed.

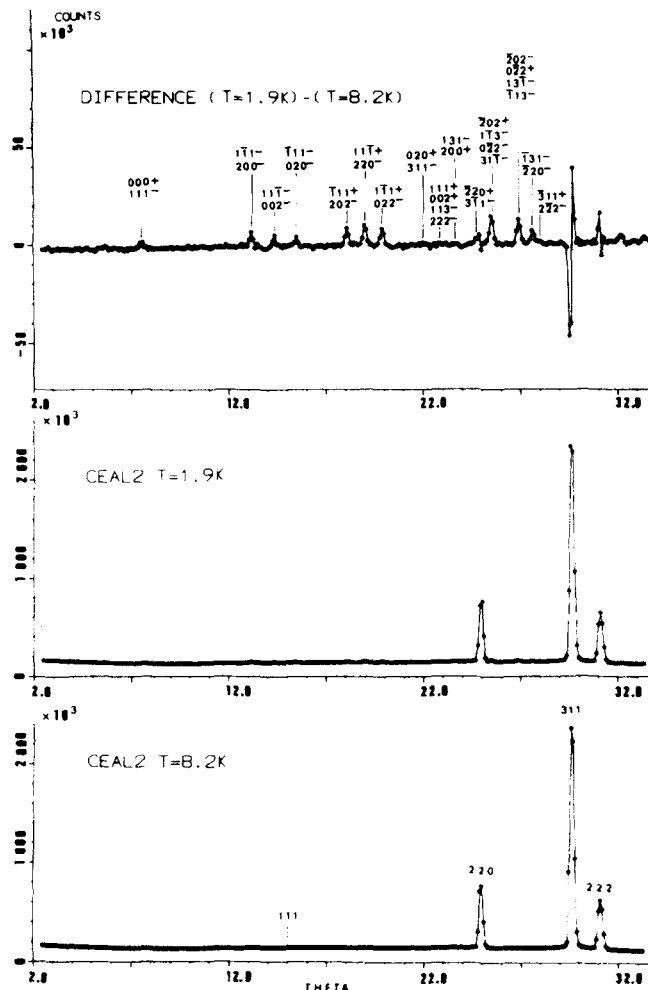


Fig. 4 Neutron diffraction patterns of  $\text{CeAl}_2$  measured at 1.9 K and 8.2 K and their difference.

### 1. Powder experiments

The powder experiments have been performed on the ultra-sensitive multidetector D1B, located on a thermal neutron guide tube of I.L.L. high flux reactor. This diffractometer allows simultaneous recording of  $80^\circ$  of the diffraction patterns.

Two different diagrams (between  $2\theta = 5^\circ$  and  $2\theta = 85^\circ$ ) have been recorded [13], above ( $T = 8.2$  K) and below ( $T = 1.9$  K) the temperature of the transition ( $T = 3.8$  K). The wavelength was 2.397 Å. At  $T = 8.2$  K only the nuclear peaks are present, but at  $T = 1.9$  K numerous but very weak extra lines appear. They are clearly shown in the difference pattern (figure 4). These magnetic lines correspond to a magnetic cell not commensurate with the chemical one ; they have been identified as first order satellites of the propagation vector :

$$\vec{k} = (1/2 + \tau, 1/2 - \tau, 1/2) \quad \text{with } \tau = 0.112 (1).$$

The experimental intensities of the magnetic satellites are compared with the calculated ones for different models of magnetic structure. The best agreement corresponds to a modulated structure with the moments along  $[111]$  and an antiparallel ordering of the two Bravais lattices corresponding to Ce atoms in (000) and  $(1/4, 1/4, 1/4)$  (figure 5). The maximum value of the moment is 0.89 (0.05)  $\mu_B$ . This structure can be described by antiferromagnetic (110) planes together with a modulation perpendicular to those planes.

However, due to the weakness of the magnetic lines, possible higher order satellites could not be detected by this powder experiment. A more accurate experiment

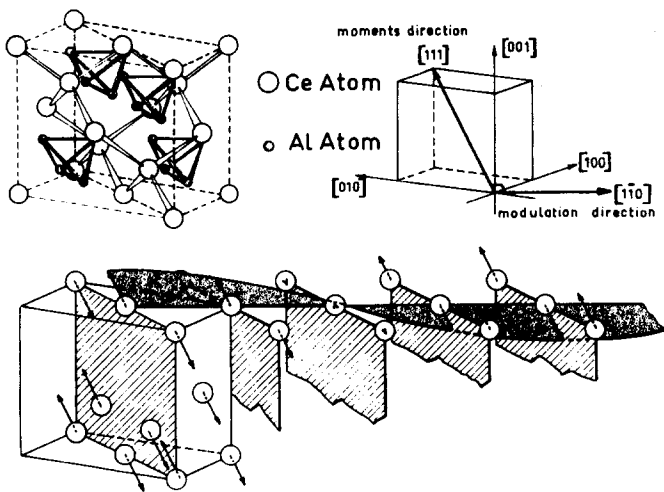


Fig. 5 Crystallographic and magnetic structure of  $\text{CeAl}_2$ . The magnetic structure consists of type II antiferromagnetic planes (110) with moments along [111] (hatched planes) with a transverse modulation along [110]. The moments of the atoms (0,0,0) and  $(1/4, 1/4, 1/4)$  are antiparallel.

was therefore necessary. On the other hand the value of the temperature ( $T = 1.9 \text{ K} \sim T_N/2$ ) is not low enough in order to characterize the ground state of  $\text{CeAl}_2$ .

### 2. Single crystal experiment

An experiment has been done on a large single crystal ( $0.4 \text{ cm}^3$ ) and at very low temperature ( $T \sim 0.4 \text{ K} \sim T_N/10$ ) using a  $\text{He}^3$  cryostat. Neutron diffraction measurements were performed on the DN3 diffractometer at the Siloe reactor of the C.E.N. Grenoble. To obtain the magnetic reflections from a single crystal the different magnetic domains must be considered by studying the number of equivalent  $k$  vectors. In  $\text{CeAl}_2$  the  $k$  vectors are on the first Brillouin zone boundary (figure 6) and there is 24 components in the star of  $k$ . The corresponding magnetic satellites are presented in figure 6 for the A zone. A scan in the  $l = 0.5$  plane along a diagonal of A zone from  $(3, -2, 1/2)$  to  $(2, -1, 1/2)$  goes through the positions of two first order and two third order satellites. Such scans are presented in figure 7 at  $T = 0.42 \text{ K}$  and  $T = 1.53 \text{ K}$  together with partial scans for other temperatures. The first order satellites allow the determination of  $\tau$ . Its value ( $\tau = 0.110(2)$ ), in good agreement with the powder results, is constant within experimental errors (figure 8). The third order satellites expected in the hypothesis of a squaring up of the sinusoidal structure would appear in position indicated by an arrow in figure 7. Their estimated intensities, approximately  $1/10$  of the corresponding first order satellites, are indicated by dotted lines. Such reflections are absent and they have not been observed for a number of different scans at  $T = 1.5 \text{ K}$  nor at  $T = 0.4 \text{ K}$ . This result shows clearly that the sine wave modulation remains stable down to very low temperature. The only variation concerns the intensities of the magnetic satellites which decrease slowly from  $1.5 \text{ K}$  to reach zero near  $3.8 \text{ K}$  (figure 8), the transition temperature of  $\text{CeAl}_2$ .

### 3. Group theory

The modulated structure found for  $\text{CeAl}_2$  is compatible with the symmetry considerations resulting from group theory. Actually the space group of the crystal structure is  $\text{Fd}3m$  with 2 Bravais lattices in (000) and  $(1/4, 1/4, 1/4)$ . The only symmetry elements leaving  $k$  invariant are the identity (E) and a twofold axis ( $C_{2b}$ ) parallel to  $[1\bar{1}0]$ . The  $G_k$  group constituted from E and  $C_{2b}$  has two one dimensional representations

$\Gamma_1$  and  $\Gamma_2$  and the 6 dimensional representations  $\Gamma$  of the components  $m_{k,1}^{(1)}$  and  $m_{k,i}^{(2)}$  of the magnetic moments of 2 Bravais lattices can be decomposed in  $\Gamma = 3(\Gamma_1 + \Gamma_2)$ . It is possible to show [19] that the general solution for the magnetic structure is not collinear but that one may obtain collinear modulated structures :

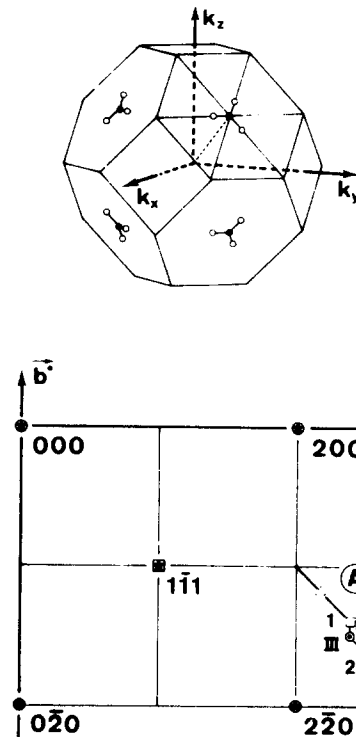


Fig. 6 Brillouin zone and reciprocal lattice of  $\text{CeAl}_2$ . On the 1<sup>st</sup> Brillouin zone boundary (upper part) the extremity of equivalent propagation vectors are represented by open circles ; the full circles correspond to the equivalent  $(1/2, 1/2, 1/2)$  points. In the reciprocal lattice perpendicular to  $[001]$  (lower part) the magnetic reflections are presented in the A zone. Three of them (circles I, II, III) correspond to  $(220)$  nuclear reflection with three propagation vectors :

$$\vec{k}_1 = \frac{1}{2} + \tau, \frac{1}{2} - \tau, \frac{1}{2}; \vec{k}_2 = \frac{1}{2}, \frac{1}{2} + \tau, \frac{1}{2} - \tau;$$

$$\vec{k}_3 = \frac{1}{2} - \tau, \frac{1}{2}, \frac{1}{2} + \tau$$

and the three others (squares 1, 2, 3) correspond to  $(3\bar{1}1)$  nuclear reflections with the propagation vectors  $-\vec{k}_1, -\vec{k}_2, -\vec{k}_3$ . These magnetic reflections are in  $l = 0.39$  (■, ●),  $l = 0.50$  (□, ○) and  $l = 0.61$  (▣, ⊙). The triangles indicate, for  $l = 0.50$ , the positions of the third order satellites in the case of an anti-phase structure.

i) a longitudinal modulated structure with moment parallel to  $[1\bar{1}0]$ , ii) transverse modulated structures with moments perpendicular to  $[1\bar{1}0]$ . In both cases the coupling between the 2 Bravais lattices is either parallel or antiparallel. The magnetic structure found for  $\text{CeAl}_2$  with a transverse modulation and magnetic moments parallel to  $[111]$  corresponds to the second of the possible cases.

### III. CONDITIONS FOR THE EXISTENCE OF A MODULATED MAGNETIC STRUCTURE IN $\text{CeAl}_2$

Three conditions are necessary for a modulated structure : i) A competition between positive and negative long range interactions. This corresponds to

a maximum of the Fourier transform of exchange interactions  $J(q)$  for  $q \neq 0$ . ii) An anisotropy large enough to produce a preferential direction for the magnetic moment and consequently to favour a modulated rather than an helical magnetic structure. iii) A possibility of reduction of the magnetic moments. These three conditions are now discussed in the case of  $CeAl_2$ .

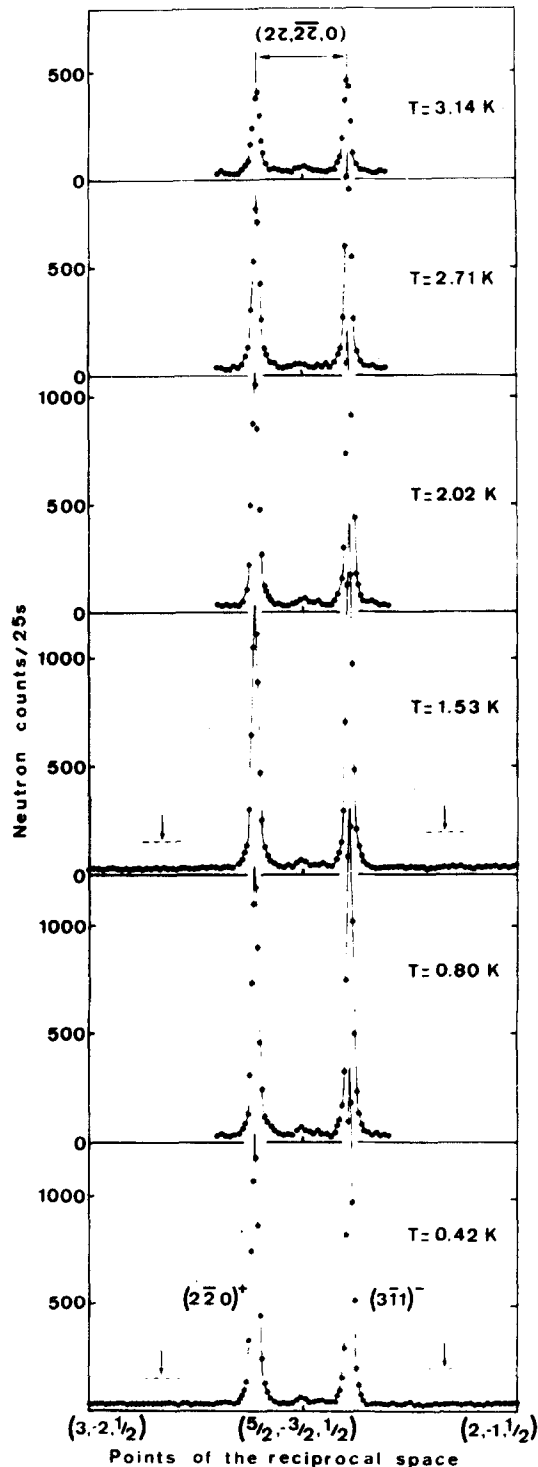


Fig. 7 Scan along the diagonal line of the A square (see figure 6) at different temperatures. Positions and intensities of the third order satellites in the case of an antiphase structure are indicated by arrows and dotted lines respectively.

### 1. Exchange interactions

Magnetization [20] and neutron diffraction measurements [21] have shown that the  $RAI_2$  compounds are all ferromagnetic except  $YbAl_2$  which is not ordered and  $CeAl_2$ . On the one hand, in field less than 50 kOe, the qualitative features of the magnetization of  $CeAl_2$ , similar to those of an antiferromagnetic, show the existence of negative long range interactions [4]. On the other hand the extrapolation to  $x = 0$  of the Curie temperature of the alloy  $Pr_xCe_{1-x}Al_2$  [22] seems to indicate that strong positive interactions exist in  $CeAl_2$ .

The magnetic structure confirms the coexistence of both types of interaction. However the origin of a strong negative long range interaction needed to stabilize the essentially antiferromagnetic structure found for  $CeAl_2$  is unknown. It could be associated with resonant exchange, as the negative sign of  $J$  is.

### 2. Anisotropy

The anisotropic character observed on single crystals of  $CeAl_2$  in an applied field is evident from magnetization measurements [4] and confirmed by specific heat measurements [23]. However, the  $\Gamma_7$  crystal field ground state is isotropic. The observed anisotropy is induced by the field.

The magnetic structure implies a large anisotropy even at zero applied field, possible only if the exchange field is itself sufficient to induce this anisotropy.

This result may be demonstrated by a detailed calculation of the anisotropy of  $CeAl_2$  performed by using a crystal field model for a two sublattices antiferromagnet [6]. From this calculation, a molecular field coefficient  $\lambda$  ( $\lambda =$  sum of the exchange coefficients  $\lambda_A$  between sublattices and  $\lambda_F$  inside each of them), corresponding to a Néel temperature of about 6.5 K, is sufficient to induce an anisotropy energy of the same order of magnitude as the exchange one.

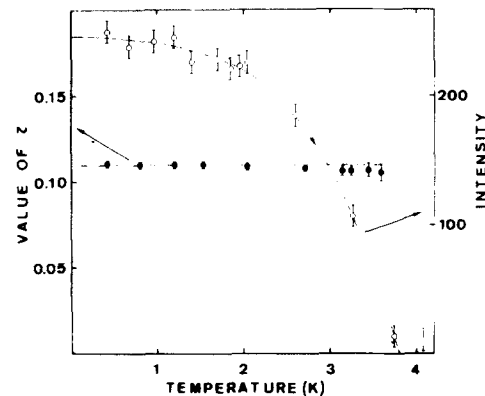


Fig. 8 Thermal variation of  $\tau$  (involved in the propagation vector) and of the intensity of the  $(111)^+$  satellite.

### 3. Nature of the ground state

The modulation of the magnetic structure obtained implies also that the magnetic moments associated with some sites of  $Ce^{3+}$  have amplitudes smaller than that corresponding to the  $\Gamma_7$  Kramers' doublet. Given the very low temperature reached in the neutron experiment ( $T \sim T_N/10$ ) this cannot be a thermal effect as according to Elliott [24] and Kaplan [25]. Such effects are possible only near  $T_N$ . This result constitutes therefore a violation of the concept of Kramers' degeneracy in metals. It is obviously due to the interaction with conduction electrons.

Before proceeding it is appropriate to remark that modulated magnetic structures can remain stable down to zero Kelvin for non Kramers' ions [26]. For instance, as shown for  $TbNi_{0.6}Cu_{0.4}$  [27], the reduction of the magnetic moment may occur at low temperature without

loss of entropy on condition that the crystal field ground state is non magnetic.

In the case of the  $Ce^{3+}$  Kramers' ion the crystal field ground state cannot be non magnetic. However strong coupling  $-\mathcal{J}S_G^z$  of the cerium spin  $S$  with the conduction electrons spins  $\sigma$  may lead to a new ground state. The coupling constant  $\mathcal{J}$  being negative in  $CeAl_2$  (see paragraph II) the ground state, which is a  $\Gamma_7$  doublet in the ionic representation may become a singlet in the metal [28]. A magnetic field mixes the singlet with the excited magnetic states. Such a mixing will result in zero applied field from the molecular field due to long range  $Ce^{3+} - Ce^{3+}$  exchange interactions. The cerium magnetic moments are then intermediate between zero (for  $\lambda < J^2 \ll kT_K$ ,  $T_K$ : Kondo temperature), and a maximum value (for  $\lambda < J^2 \gg kT_K$ ). The molecular field may be different from site to site (see paragraph III.1) and gives a modulated structure.

In this description, the ground state of  $Ce^{3+}$  in  $CeAl_2$  arises from the competition between exchange interactions (tending to antiferromagnetic ordering) and a Kondo effect (tending to vanishing of the  $Ce^{3+}$  magnetic moment). This implies a Kondo temperature comparable to the ordering one (characteristic of the exchange energy), i.e. of some Kelvins.

#### IV. COMPETITION BETWEEN THE KONDO EFFECT AND MAGNETIC ORDERING

In order to estimate the value of the Kondo temperature in  $CeAl_2$ , we examine below some of its properties such as magnetization and specific heat, and we relate these properties to theoretical models. Three main types of theoretical approach exist. i) A one dimensional Kondo lattice treated in a mean field approximation [29] and later completed by a renormalization technique [30]. ii) A phenomenological "resonance level" model [31] recently developed [5,32,33]. iii) A standard calculation [34], starting from that of Schlottmann [35] describing single impurity Kondo properties, and extrapolated to concentrated systems.

In all these models an ordered state is obtained for low values of  $\mathcal{J}$  and a Kondo state for large values of  $\mathcal{J}$ . Moreover the magnetization at  $T = 0$  K is always

expressed as a function of the Kondo temperature by an expression of the type :

$$m/m_0 = 2/\pi \text{Arctg} \left[ \frac{\lambda}{\Delta} \frac{m}{m_0} \right] \quad (1)$$

where the remaining undefined parameters are  $m_0 = g_J \mu_B \langle J^z \rangle$ , the moment of the initial doublet, and  $\Delta = kT_K$ .

#### 1. Evaluation of the Kondo temperature from measurements under hydrostatic pressure

The magnetization curves  $M(H)$  were measured at 1.7 K under hydrostatic pressure up to 6 kbar, with the field parallel to the [111] axis of a single crystal [36]. They decrease when the pressure goes up (figure 9). A linear extrapolation of the  $M(P)$  variation indicates a non magnetic state at about 40 kbar.

According to expression (1) the magnetization decreases at 0 K when  $T_K$  increases. Such a variation would be important only if  $\Delta \sim \lambda$ . This leads to two consequences for  $CeAl_2$ : i) the Kondo temperature increases with pressure, ii) the two temperatures  $T_K$  and  $T_N$  are close to 4 K. The increase of  $T_K$  with pressure ( $T_K \propto (\rho \mathcal{J})^{-1/\rho \mathcal{J}}$  [34]) is a consequence of an augmentation of both the density of state at the Fermi level  $\rho$  and of the exchange coupling  $\mathcal{J}$  [36,34]. The exchange  $\mathcal{J}$  increases because of the larger admixture of conduction band state with the 4f level, while  $\rho$  gets larger due to decrease in the volume available for conduction electrons. This last effect, negligible for the delocalized s electrons, becomes important for the 5d electrons which are localized in the  $Ce^{3+}$  "sphere" (see paragraph II). In particular the large difference in the Kondo temperatures of  $CeAl_2$  and  $CeLaAl_2$  [37] must be associated with the d-character of conduction electrons.

By resistivity and specific heat measurements a similar value has been found for the Kondo temperature of  $CeAl_2$  ( $T_K = 5 \pm 2$  K) [38,5].

Associated with the reduction of the moment at 0 K a reduction of the Néel temperature is expected [34]. This has been evaluated from the function  $T_K(\rho \mathcal{J})$  and  $T_N(\rho \mathcal{J})$  given by the model iii) (figure 10). Using the variation of  $\rho \mathcal{J}$  with pressure [39] it is possible to obtain the curve  $d \ln T_N / dP$  as a function of  $\rho \mathcal{J}$  (insert of figure 10). The experimental value deduced from the susceptibility measured under pressure (insert of figure 9) gives a value of  $\rho \mathcal{J}$  and so the Kondo temperature is found here close to 7 K and the reduction of the Néel temperature is  $T_N/T_{N0} = 0.65$ . In the absence of the Kondo effect, the Néel temperature would be near 6 K.

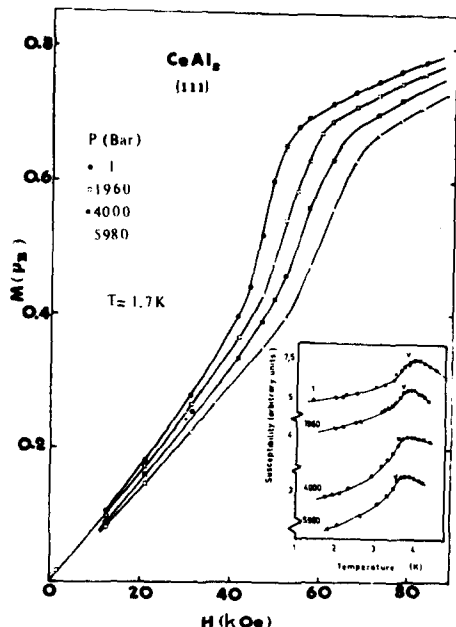


Fig. 9 Magnetization curves under pressure measured along the [111] axis of a single crystal of  $CeAl_2$  [36]. The insert shows the thermal variation of the initial susceptibility for the same hydrostatic pressures [34]. The Néel temperature is indicated by an arrow.

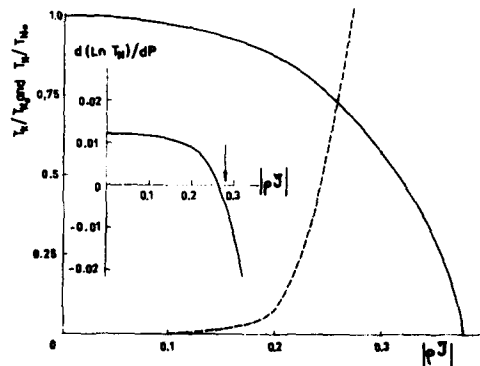


Fig. 10 Variations of the normalized Kondo and ordering temperatures,  $(T_K/T_{K0} \text{---})$  and  $(T_N/T_{N0} \text{—})$ , with the product of the density of states at the Fermi energy and the s-f exchange constant  $(\rho \mathcal{J})$  [34]. Insert: relative pressure induced modification of the ordering temperature (in  $kbar^{-1}$ ) as a function of  $(\rho \mathcal{J})$ .



## 2. Reduction of the $Ce^{3+}$ moment

The entropy associated with a modulated magnetic structure can be written :

$$S(T) = \frac{1}{N} \sum_{n=1}^N S_n(T)$$

where  $S_n(T)$  is the entropy of the  $n^{\text{th}}$  site and  $N$  the number of sites.  $S_n(T)$  is an increasing function. On sites of large molecular field  $S_n(T)$  reaches rapidly the value  $R \ln 2$ , but such a value is obtained only at temperatures  $T \gg T_K$  on sites of low molecular field [31]. Consequently the contribution to the entropy of the sites of low molecular field (i.e. of low moment) is very small and the total entropy  $S(T)$  is smaller than  $R \ln 2$  at  $T_N$ . If one considers for simplicity from the modulated structure of  $CeAl_2$  (fig. 5) that one third of the cerium moments does not give any entropy, one finds that  $S(T_N) = (2/3)R \ln 2$ . This value has been effectively obtained from specific heat measurements (fig. 11). Such an unusual result confirms that the observed reductions of  $Ce^{3+}$  moments are intrinsic and not of thermal origin. On the other hand the reduced  $Ce^{3+}$  moments do not present any discontinuity when the temperatures go through  $T_N$ , otherwise a latent heat would be present at this temperature. These reductions of  $Ce^{3+}$  moment, observed in the paramagnetic state in zero field, would become very small at about 15 K where the total entropy is attained. At this temperature the thermal fluctuations are larger than the Kondo ones.

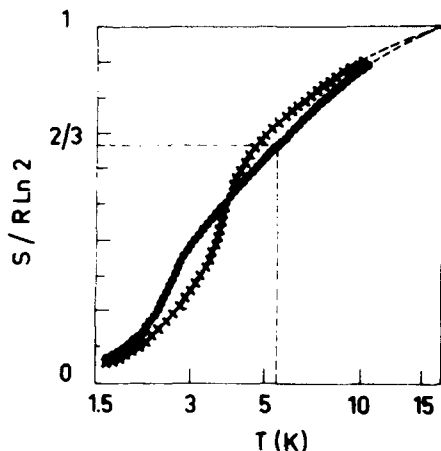


Fig. 11 Entropy per formula unit of  $CeAl_2$  as a function of temperature (obtained by Bredl et al) [5] in magnetic field  $H = 0$  (x) and  $H = 50$  kOe (•) parallel to [100].

This discussion can be extended to the specific heat measurements under magnetic fields [35]. As in zero field, the entropy curve measured at 50 kOe reaches  $R \ln 2$  at about 15 K (fig. 11). This result shows that while a magnetic field of the order of 50 kOe destroys the antiferromagnetic ordering it is not large enough to destroy the Kondo effect.

## CONCLUSION

The compound  $CeAl_2$ , where each cerium atom has the same environment, is an example of concentrated Kondo lattice. At low temperature its magnetic behaviour is the result of a competition between two contradictory processes. On the one hand the moments tend to vanish as the result of the Kondo effect. On the other hand the interactions between neighbours tend to order the magnetic moments and to reinforce them. The compromise observed in the case of  $CeAl_2$ , a modulated structure below 3.8 K, corresponds to an original solution. Original is the Kondo reduction of the magnetic moments because it does not affect in the same way all the cerium atoms of the compound. Original also is the

magnetic structure because, though  $Ce^{3+}$  is a Kramers ion, the sinusoidal modulation remains stable until very low temperatures.

## ACKNOWLEDGMENTS

We wish to thank B. Coqblin, C. Lacroix-Lyon-Caen and J. Rossat-Mignod for interesting discussions.

## REFERENCES

- J. Kondo, *Progr. Theoret. Phys. (Kyoto)* **32**, 37 (1964) and **34**, 523 (1965).
- K.H.J. Buschow and H.J. van Daal, *Phys. Rev. Lett.* **23**, 408 (1969).
- B. Cornut and B. Coqblin, *Phys. Rev.* **B5**, 4541 (1972).
- B. Barbara, M.F. Rossignol, H.G. Purwins and E. Walker, *Sol. Stat. Commun.* **17**, 1525 (1975).
- C.D. Bredl, F. Steglich and K.D. Schotte, *Z. Phys.* **B29**, 327 (1978).
- B. Barbara, R. Lagnier and M.F. Rossignol, to be published.
- I. Zoric, J. Markovics, L. Kupferberg, M. Croft and R.D. Parks, *Proc. Int. Conf. on valence instabilities and related narrow band phenomena 1976* (Ed. R.D. Parks, Plenum, New York 1977) p. 479.
- R.W. Hill and J.M. Machado da Silva, *Phys. Lett.* **30A**, 13 (1969).
- S.W. Lovesey and D.E. Rimmer, *Rep. Prog. Phys.* **32**, 333 (1969).
- G.H. Lander and T.O. Brun, *J. Chem. Phys.* **53**, 1387 (1970).
- J.P. Desclaux, private communication.
- B. Barbara, J.X. Boucherle, J.P. Desclaux, M.F. Rossignol and J. Schweizer, in "Crystal field effects in metals and alloys" (Ed. A. Furrer, Plenum Press, New York 1977) p. 168.
- R.M. Moon, W.C. Koehler, J.W. Cable and H.R. Child, *Phys. Rev.* **B5**, 997 (1972).
- J.X. Boucherle and J. Schweizer, *Physica* **86-88B**, 174 (1977).
- J.X. Boucherle, Thesis, University of Grenoble (1977).
- B. Coqblin and C.F. Ratto, *Phys. Rev.* **21**, 1065 (1968).
- V. Niclescu, I. Pop and N. Rosenberg, *Phys. Lett.* **34A**, 265 (1971).
- B. Barbara, J.X. Boucherle, J.L. Buevoz, M.F. Rossignol and J. Schweizer, *Sol. Stat. Commun.* **24**, 481 (1977).
- J. Rossat-Mignod, *Coll. Int. CNRS "La physique des terres rares à l'état métallique"*, St-Pierre de Chartreuse 1978, to appear in *J. de Physique*.
- H.J. Williams, J.H. Wernick, E.A. Nesbitt and R.C. Sherwood, *J. Phys. Soc. Japan* **17**, Suppl. B1, 91 (1962).
- N. Nereson, C. Olsen and G. Arnold, *J. Appl. Phys.* **37**, 4575 (1966) and *J. Appl. Phys.* **39**, 4605 (1968). C.E. Olsen, G. Arnold and N. Nereson, *J. Appl. Phys.* **38**, 1395 (1967).
- W.M. Swift and W.E. Wallace, *J. Phys. Chem. Solids* **29**, 2053 (1968).
- C.D. Bredl and F. Steglich, *J. of Mag. and Mag. Mat.* **7**, 286 (1978).
- R.J. Elliott, *Phys. Rev.* **124**, 346 (1961).
- T.A. Kaplan, *Phys. Rev.* **124**, 329 (1961).
- D. Gignoux, J.C. Gomez-Sal, R. Lemaire and A. de Combarieu, *Sol. Stat. Commun.* **21**, 637 (1977).
- D. Gignoux, R. Lemaire and D. Paccard, *Phys. Lett.* **41A**, 187 (1972).
- P. Nozières, *J. Low Temp. Phys.* **17**, 31 (1974).
- S. Doniach, *Physica* **91B**, 231 (1977) and *Proc. Int. Conf. Rochester 1976*, see ref. 7, p. 169.
- R. Jullien, J. Field and S. Doniach, *Phys. Rev. Lett.* **38**, 1500 (1977).
- K.D. Schotte and U. Schotte, *Phys. Lett.* **55A**, 38 (1975).

32. A. Benoît, J. Flouquet, M. Ribault, F. Flouquet, G. Chouteau and R. Tournier, *J. Physique Lettres* 39, 94 (1978).
33. A. Benoît, J. Flouquet and M. Ribault, Coll. Int. CNRS "La physique des terres rares à l'état métallique" St-Pierre de Chartreuse 1978, to appear in *J. de Physique*.
34. B. Barbara, M. Cyrot, C. Lacroix-Lyon-Caen and M.F. Rossignol, Coll. Int. CNRS "La physique des terres rares à l'état métallique" St-Pierre de Chartreuse 1978, to appear in *J. de Physique*.
35. P. Schlottmann, *J. of Mag. and Mag. Mat.* 1, 72 (1978).
36. B. Barbara, H. Bartholin, D. Florence, M.F. Rossignol and E. Walker, *Physica* 86-88B, 177 (1977).
37. S.D. Bader, N.E. Phillips, M.B. Maple, C.A. Luengo, *Sol. Stat. Commun.* 16, 1263 (1975) and references therein.
38. F. Steglich, W. Franz, W. Seuken and M. Loewenhaupt, *Physica* 86-88B, 503 (1977).
39. M. Nicolas-Francillon, A. Percheron, J.C. Achard, O. Gorochov, B. Cornut, D. Jerome and B. Coqblin, *Sol. Stat. Commun.* 11, 845 (1972).